Behavioral/Systems/Cognitive

Histamine H_3 Receptors Inhibit Serotonin Release in Substantia Nigra Pars Reticulata

Sarah Threlfell,[1] Stephanie J. Cragg,[1] Imre Kalló,[2,3] Gergely F. Turi,[3] Clive W. Coen,[2] and Susan A. Greenfield[1]

[1]Department of Pharmacology, University of Oxford, Oxford OX1 3QT, United Kingdom, [2]School of Biomedical Sciences, King's College London, London SE1 1UL, United Kingdom, and [3]Institute of Experimental Medicine, Hungarian Academy of Sciences, Budapest H-1450, Hungary

The substantia nigra pars reticulata (SNr) plays a key role in basal ganglia function. Projections from multiple basal ganglia nuclei converge at the SNr to regulate nigrothalamic output. The SNr is also characterized by abundant aminergic input, including dopaminergic dendrites and axons containing 5-hydroxytryptamine (5-HT) or histamine (HA). The functions of HA in the SNr include motor control via HA H_3 receptors (H_3Rs), although the mechanism remains far from elucidated. In Parkinson's disease, there is an increase in H_3Rs and the density of HA-immunoreactive axons in the SN.

We explored the role of H_3Rs in the regulation of 5-HT release in SNr using fast-scan cyclic voltammetry at carbon-fiber microelectrodes in rat midbrain slices. Immunohistochemistry identified a similar distribution for histaminergic and serotonergic processes in the SNr: immunoreactive varicosities were observed in the vicinity of dopaminergic dendrites. Electrically evoked 5-HT release was dependent on extracellular Ca^{2+} and prevented by Na_V^+-channel blockade. Extracellular 5-HT concentration was enhanced by inhibition of uptake transporters for 5-HT but not dopamine. Selective H_3R agonists (R)-(-)-α-methyl-histamine or immepip inhibited evoked 5-HT release by up to 60%. This inhibition was prevented by the H_3R antagonist thioperamide but not by the 5-HT_{1B} receptor antagonist isamoltane. H_3R inhibition of 5-HT release prevailed in the presence of GABA or glutamate receptor antagonists (ionotropic and metabotropic), suggesting minimal involvement of GABA or glutamate synapses. The potent regulation of 5-HT by H_3Rs reported here not only elucidates HA function in the SNr but also raises the possibility of novel targets for basal ganglia therapies.

Key words: **histamine; 5-hydroxytryptamine; basal ganglia; substantia nigra; fast-scan cyclic voltammetry; Parkinson's disease**

Introduction

The substantia nigra pars reticulata (SNr) is a strategic point for integration of inputs from the "direct" and "indirect" pathways of the basal ganglia (Alexander and Crutcher, 1990). It also provides a major output projection from the basal ganglia to the thalamus, where it influences the activity of the thalamocortical relay. Among the inputs to the SNr is a projection from histamine (HA)-containing neurons of the tuberomammillary nucleus (Panula et al., 1989). Although there is limited information on the actions of HA in the SNr, HA has been implicated in the modulation of GABA release at striatonigral synapses (Garcia et al., 1997) and in the local regulation of motor functions (Garcia-Ramirez et al., 2004). In Parkinson's disease (PD), there is an increase in HA levels and in the varicosity size and density of HA fibers in the SN (Anichtchik et al., 2000a). Furthermore, H_3R binding density is elevated in the SN in PD (Ryu et al., 1994; Anichtchik et al., 2000b, 2001) and in rats after 6-OHDA lesions (Ryu et al., 1994; Anichtchik et al., 2000b, 2001).

Three HA receptors have been identified in the CNS, of which two, H_2 and H_3, are found at high densities in the basal ganglia (Vizuete et al., 1997; Pillot et al., 2002). H_3 binding sites are particularly abundant in the SNr, but there is only low expression of the mRNA for H_3Rs (Pillot et al., 2002). These findings indicate that H_3Rs are principally expressed by afferents to and not local projection neurons within the SN. Regions that express H_3R mRNA and project to the SNr include the striatum, subthalamic nucleus, and raphe nuclei but not the dopaminergic neurons in the substantia nigra pars compacta (SNc)–ventral tegmental area (Pillot et al., 2002).

The H_3R is predominantly a presynaptic receptor that has been shown to inhibit release of HA (Arrang et al., 1983), glutamate (Brown and Reymann, 1996; Brown and Haas, 1999; Molina-Hernandez et al., 2001), GABA (Garcia et al., 1997; Yamamoto et al., 1997; Arias-Montano et al., 2001), norepinephrine (Schlicker et al., 1989, 1992, 1999), dopamine (DA) (Schlicker et al., 1993), acetylcholine (Arrang et al., 1995; Giorgetti et al., 1997; Prast et al., 1999), and 5-hydroxytryptamine (5-HT) in cortex (Schlicker et al., 1988; Fink et al., 1990). The present study was designed to elucidate the role of H_3 receptors (H_3Rs) in the SNr. We initially used immunohistochemical techniques to establish whether there is a comparable distribution of histaminergic and serotonergic processes in the SNr. We then used fast-scan cyclic voltammetry (FCV) at carbon-fiber microelectrodes (CFMs) to monitor in real time the modulation of electrically evoked 5-HT release in the SNr by H_3R ligands.

Received July 7, 2004; revised Aug. 18, 2004; accepted Aug. 20, 2004.

This work was supported by Novartis Pharma AG, The Wellcome Trust, and Beit Memorial Research Fellowship (S.J.C.). We are grateful to Drs. Kelly Allers and Csaba Fekete for expert advice and critical reading of this manuscript.

Correspondence should be addressed to Dr. Stephanie J. Cragg, Department of Pharmacology, University of Oxford, Mansfield Road, Oxford OX1 3QT, UK. E-mail: stephanie.cragg@pharm.ox.ac.uk.

DOI:10.1523/JNEUROSCI.2690-04.2004

 0270-6474/04/248704-07$15.00/0

Materials and Methods

Tissue preparation for immunohistochemistry. Adult male Wistar rats (150–180 gm; Charles River Laboratories, Isaszeg, Hungary) were maintained for 1 week in a light- and temperature-controlled environment (lights on 5:00 A.M. to 7:00 P.M.; 22 ± 1°C) and allowed access to food and water *ad libitum*. To enhance detection of histamine-containing processes, synthesis of brain histamine was stimulated (Schwartz et al., 1972; Prell et al., 1996) by L-histidine loading (6 mM, i.p.; $n = 3$) 1 hr before transcardial perfusion with 50 ml of phosphate buffered 4% 1-ethyl-3(3-dimethylaminopropyl)-carbodiimide (EDCDI; Sigma, Poole, UK) under pentobarbital anesthesia (80 mg/kg); the brains were removed and immersed in EDCDI (4 d) followed by 2% paraformaldehyde (PFA) (1 d). For the immunohistochemical detection of serotonergic processes, animals ($n = 3$) were perfused transcardially with 4% PFA in 0.1 M PBS under pentobarbital anesthesia (80 mg/kg); the brains were removed and postfixed in 2% PFA. All brains were infiltrated in 30% sucrose overnight; midbrain sections (25 μm) were cut in the coronal plane using a freezing microtome (Leica, Vienna, Austria).

Immunohistochemistry. Pretreatment of sections included sequential incubation in 0.5% Triton X-100 (30 min), 0.5% H_2O_2 (10 min), and 2% normal horse serum (30 min). The procedure used to detect histamine-immunoreactive processes required EDCDI fixation (Panula et al., 1984). Serotonergic processes were identified with antibodies against the serotonin transporter (SERT) in PFA-fixed sections. Tyrosine hydroxylase (TH) immunoreactivity (IR) served to identify dopamine-containing structures following either form of fixation.

For double-label immunohistochemical detection of HA-IR together with TH-IR, sections were initially incubated in rabbit anti-histamine (Panula et al., 1984) (1:12,000) for 72 hr at 4°C. Biotinylated donkey anti-rabbit IgG (1:1000; Jackson Laboratories, Bar Harbor, ME) and the ABC solution (1:1000; Vector Laboratories, Burlingame, CA) were used before amplification (Adams, 1992) with biotinylated tyramide (1:1000); sections were then incubated overnight at 4°C in Alexa 594 streptavidin (1:500; Molecular Probes, Eugene, OR). Subsequently, mouse anti-TH [monoclonal antibody (mAb) 22941, 1:1000; Incstar, Stillwater, MN] was applied for 48 hr at 4°C; this was visualized with Alexa 350 conjugated to goat anti-mouse IgG (1:500, overnight at 4°C; Molecular Probes).

For double-label immunohistochemical detection of SERT together with TH-IR, mouse anti-SERT (mAb 1564, 1:2000; Chemicon, Temecula, CA) was applied for 48 hr at 4°C and visualized using black silver–gold intensified nickel diaminobenzidine (SGI-NiDAB) as described previously (Kalló et al., 2001). Subsequently, mouse anti-TH (mAb 22941, 1:1000; Incstar) was applied for 48 hr at 4°C and detected by the brown DAB reaction product. Previous studies (Liposits et al., 1986) have demonstrated that double-label peroxidase-based immunohistochemistry can be successfully performed using primary antibodies from the same species when the first reaction product is silver–gold intensified.

Sections were mounted, and a coverslip was fixed with DPX (a mixture of distyrene, tricresyl phosphate, and xylene; Fluka, Buchs, Switzerland) for the SGI-NiDAB/DAB sections or with Antifade (Molecular Probes) for the immunofluorescence sections and examined using an Axiophot microscope (Zeiss, Göttingen, Germany) equipped with a real-time Spot digital camera (Diagnostic Instruments, Sterling Heights, MI).

Slice preparation for FCV. Male Wistar rats (150–220 gm) were anesthetized with halothane and decapitated, and their brains were removed. Midbrain slices were prepared according to methods described previously (Cragg et al., 1997b, 2002). A block of midbrain was mounted onto a specimen plate with cyanoacrylate adhesive and placed in the double-walled buffer tray in the Leica VT1000S vibratome. The buffer tray was then surrounded by ice and filled with ice-cold HEPES ringer containing the following (in mM): 120 NaCl, 5 KCl, 20 $NaHCO_3$, 6.7 HEPES acid, 3.3 HEPES salt, 2 $CaCl_2$, 2 $MgSO_4$, 1.2 KH_2PO_4, and 10 glucose saturated with 95% O_2/5% CO_2. Slices 350 μm thick were cut and maintained in individual vials in HEPES ringer for ≥ 1 hr at room temperature before transferal to the recording chamber. The coordinates of midbrain slices containing the SNr correspond to anterior 3.2–4.2 mm of adult rat, according to the atlas of Paxinos and Watson (1982). The slices were equilibrated with the superfusion medium of the recording chamber at 30–32°C for an additional 30 min before the beginning of the experiment. The superfusion medium was a bicarbonate-buffered artificial CSF (aCSF) maintained at 30–32°C and contained the following (in mM): 124 NaCl, 3.7 KCl, 26 $NaHCO_3$, 2.4 $CaCl_2$, 1.3 $MgSO_4$, 1.3 KH_2PO_4, and 10 glucose with saturated 95% O_2/5% CO_2. Ca^{2+}-free solutions included 1 mM EGTA and 2.4 mM $MgCl_2$. Superfusion flow rate was ~1.5 ml/min.

Voltammetry and carbon fiber microelectrodes. All recordings were made using a Millar Voltammeter (P.D. Systems, West Molesey, UK) as described previously (Cragg et al., 1997a,b, 2002). The instrument was used as a three-electrode potentiostat, with an Ag/AgCl wire as the reference electrode and the stainless steel flow outlet of the bath as the auxiliary. Voltammograms were obtained in the simple triangle wave mode with a voltage ramp of −0.7 to +1.3 V and then back to −0.7 V versus Ag/AgCl at a scan rate of 800 V/sec. The scan was switched out of circuit between scans. Sampling frequency was 8 Hz. Evoked extracellular concentrations of 5-HT ($[5\text{-HT}]_o$) were measured using FCV with CFMs beveled to a point (fiber tip diameter, ~6 μm; exposed fiber length, ~30 μm; MPB Electrodes, London, UK). CFMs were positioned 50–100 μm into the tissue with the aid of a binocular microscope.

Electrode calibrations were performed after the experiment in the recording chamber at 32°C using 0.25 μM 5-HT made up in all experimental solutions. Calibration solutions were made immediately before use from stock solutions of 5-HT in 0.1 M $HClO_4$. Electrode sensitivity was determined after use, and these postslice calibration factors were used to calculate $[5\text{-HT}]_o$. Sensitivity varied with electrode from 10–28 nA/μM. The minimum detection limit for 5-HT was ~15–20 nM (twice the amplitude of noise). Peak $[5\text{-HT}]_o$ detected in the SNr after 20 pulse, 100 Hz stimulation was typically 60–150 nM.

Electrical stimulation. Concentric bipolar stimulating electrodes (FHC, Bowdoinham, ME) were used to electrically evoke 5-HT release in the SN. The stimulating electrode was positioned on the tissue surface ~50–100 μm from the CFM with the aid of a binocular microscope. Stimulus pulses (0.2 msec duration; 0.6 mA) were applied in trains of 20 pulses at 100 Hz at repeat intervals of 5 min; by this time, release is fully reproducible and can be maintained for ≥2 hr. In initial experiments to characterize 5-HT release, the dependence on pulse frequency and number was verified using either trains of 20 pulses at 10–200 Hz in random order or 1–50 pulses at 100 Hz.

Drugs. Drugs were dissolved in water, aqueous alkali [(*S*)-(±)-amino-4-carboxy-methyl-phenylacetic acid (MCPG)], or acid [4-(8-methyl-9H-1,3-dioxolo[4,5-h][2,3]benzodiazepin-5-yl)-benzenamine hydrochloride (GYKI 52466)] to make stock aliquots at 1000× or 10,000× final concentrations and stored at −20°C until required. Stock aliquots were diluted with aCSF to final concentration immediately before use and perfused for >7 min before data were included in drug analysis. D-AP-5, GYKI 52466 hydrochloride, tetrodotoxin (TTX), saclofen, (*S*)-MCPG, citalopram hydrobromide, isamoltane hemifumarate, immepip dihydrobromide, and thioperamide maleate were obtained from Tocris Cookson (Bristol, UK). [1-(2-(Bis-(4-fluorophenyl)methoxy)ethyl)-4-(3 phenylpropyl)piperazine dihydrochloride] (GBR 12909) was obtained from Research Biochemicals International (Natick, MA). All other compounds were obtained from Sigma.

Data analysis and statistics. Data were acquired and analyzed using Strathclyde Whole Cell Program (University of Strathclyde, Glasgow, Scotland, UK). Current sampled at the 5-HT oxidation peak potential was measured from the baseline of each voltammogram to provide profiles of $[5\text{-HT}]_o$ versus time. This procedure minimizes inclusion of contributions from other electroactive and nonelectroactive species to the neurotransmitter oxidation current (Rice and Nicholson, 1989; Venton et al., 2003). Illustrated data represented are means ± SEM (n = number of observations). Three to five animals were used in each experiment. Illustrated voltammograms have background current subtracted. Comparisons for differences in means were assessed for parametric data by one-way ANOVA followed by *post hoc* multiple comparison *t* tests (Dunnett's); nonparametric or normalized data were compared by unpaired Mann–Whitney *U* tests (M-WU) or where appropriate by Kruskal–Wallis variance analysis followed by Dunn's *t* tests. Concentration–response

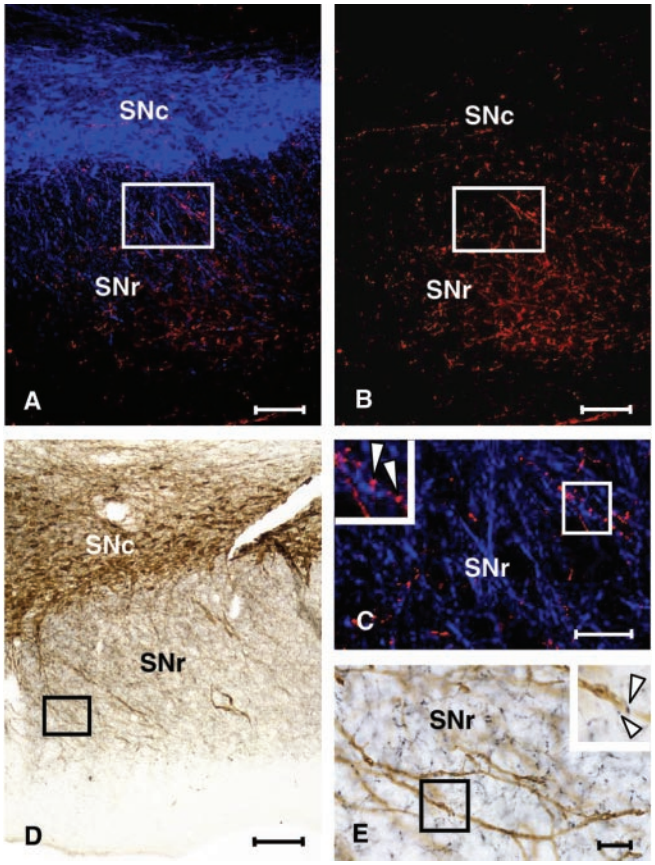

Figure 1. Photomicrographs of the SNc and SNr of rats showing immunoreactivity for histamine together with TH using fluorescence microscopy (*A–C*) and the serotonin transporter together with TH, using bright field microscopy (*D*, *E*). *A*, Low-power image of histamine-IR (with Alexa 594; red) and TH-IR (with Alexa 350; blue). *B*, Histamine-IR alone (in the same field shown in *A*). *C*, An enlarged image of the boxed area (in *A*, *B*) showing histamine-IR (red) and TH-IR (blue) in the SNr; the inset presents the boxed area (in *C*) at higher power (arrowheads indicate varicosities with histamine-IR in the vicinity of dendritic processes containing TH-IR). *D*, Low-power image of serotonin transporter-IR (black profiles) and TH-IR (brown profiles). *E*, An enlarged image of the boxed area (in *D*). Serotonin transporter-IR (black profiles) and TH-IR (brown profiles) in the SNr; the boxed area (in *E*) is shown at higher power as an inset (arrowheads indicate varicosities with serotonin transporter-IR in the vicinity of dendritic processes containing TH-IR). Scale bars: *A*, *B*, *D*, 100 μm; *C*, *E*, 50 μm.

curves were generated with GraphPad Prism software (GraphPad Software, San Diego, CA) using nonlinear regression to a sigmoidal dose–response (variable slope) from which IC_{50} values were obtained and, where appropriate, compared statistically. Statistical significance was considered as $p < 0.05$.

Results

Identification of HA and 5-HT immunoreactivity in SNr

In sections from rats perfused with EDCDI, abundant processes immunoreactive for HA or TH were observed in the SNr (Fig. 1*A–C*). Varicosities immunoreactive for HA were found in the vicinity of TH-immunoreactive processes (Fig. 1*C*). After PFA fixation, processes immunoreactive for SERT were found throughout the SNr (Fig. 1*D*,*E*). As in the case of HA-IR, SERT-immunoreactive varicosities were found in the vicinity of TH-immunoreactive processes (Fig. 1*E*). By reference to TH-immunopositive processes, we conclude that within the SNr, there is similarity in the distribution of putative terminal fields containing HA or 5-HT. Analysis of the direct ultrastructural interactions between HA-IR and 5-HT-IR is not currently feasible because of the different methodological conditions required to reveal them.

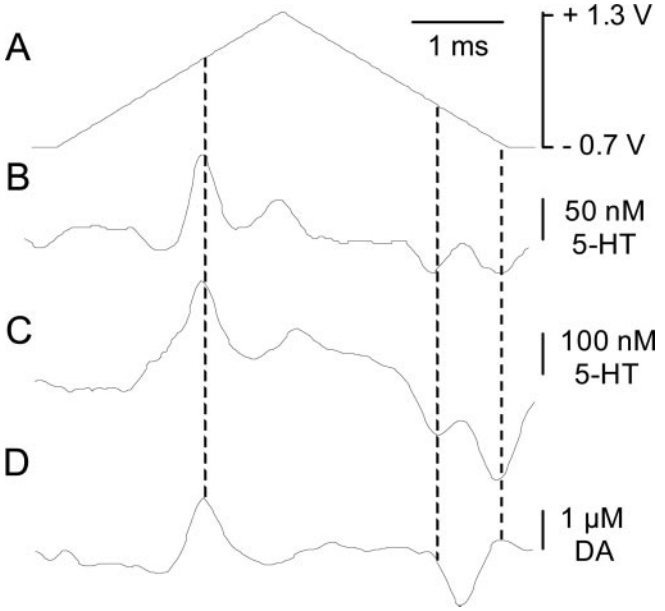

Figure 2. Voltammograms for evoked 5-HT release in SNr compared with exogenous 5-HT and DA. *A*, Scan waveform applied at a sampling frequency of 8 Hz versus Ag/AgCl. *B*, Typical current profile, or voltammogram, of 5-HT release evoked by 20 pulses at 100 Hz in SNr. Note that single oxidation and double-reduction current peaks with peak potentials of +620, −20, and −670 mV, respectively (dotted lines), that are characteristic of 5-HT (*C*) in an applied solution but not dopamine (*D*). Peak $[5\text{-HT}]_o$ in *B* corresponds to 109 nM. *C*, Calibration voltammogram for 5-HT (250 nM; sensitivity, 20 nA/μM). *D*, Calibration voltammogram for DA (2 μM; sensitivity, 3.2 nA/μM) shows characteristic oxidation and single reduction peaks at potentials of +620 and −320 mV, respectively.

Electrochemical characterization of 5-HT release in SNr

Electrical stimulation (20 pulses, 100 Hz) in SNr evoked the release, followed by the rapid removal, of an electroactive substance that could be identified as 5-HT. The voltammogram of the released substance was readily identified as 5-HT because of an oxidation peak potential at approximately +600 mV (vs Ag/AgCl) and a dual reduction profile with peak potentials at ~0 and −680 mV (Fig. 2*A*,*B*), identical to those obtained in calibration with application of 5-HT (Fig. 2*C*). The substance can readily be distinguished from DA (Fig. 2*D*) by the characteristic double-reduction current profile for 5-HT as noted previously in SNr (Davidson and Stamford, 1996; Cragg et al., 1997b; Iravani and Kruk, 1997; Bunin et al., 1998). Furthermore, it has been identified previously that the primary substance detected in rat SNr using this method is 5-HT and not DA (Cragg et al., 1997b; Iravani and Kruk, 1997; Bunin et al., 1998).

To further confirm the identity of the electrochemical signal as 5-HT and not DA, uptake inhibitors for the SERT and the DA transporter (DAT) were applied. Bath application of the SERT inhibitor citalopram (75 nM) prolonged the extracellular lifetime of 5-HT and significantly enhanced $[5\text{-HT}]_o$ (Fig. 3*A*) (M-WU; $p < 0.001$; $n = 28$) as shown previously with SERT inhibitors in the SNr (Iravani and Kruk, 1997; Bunin et al., 1998). Conversely, application of the DAT inhibitor GBR 12909 (1 μM) had no effect on the lifetime or peak concentration of the detected substance, 5-HT (Fig. 3*B*) (M-WU; $p > 0.05$; $n = 14$).

Ionic and depolarization sensitivity

Evoked release of 5-HT was apparently abolished by inhibition of voltage-gated Na^+ channels (Na_v^+) by TTX (1 μM) (Fig. 3*C*)

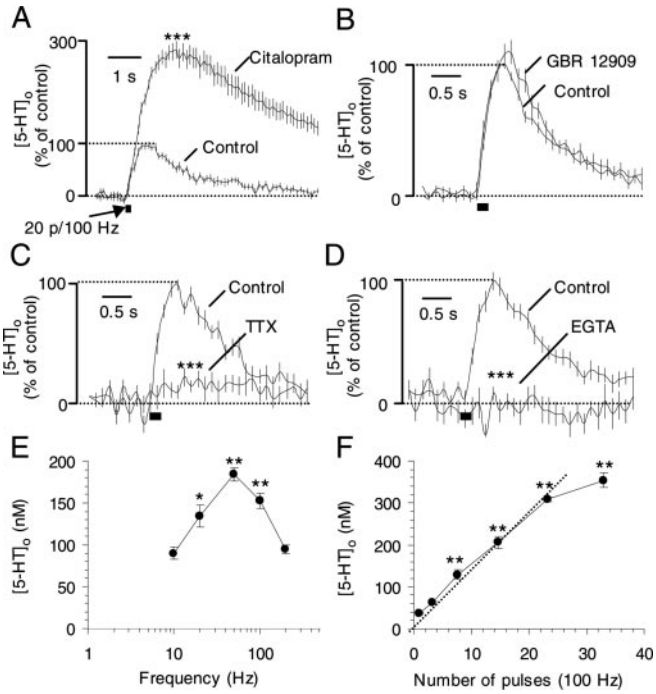

Figure 3. Release and uptake characteristics of evoked 5-HT release in SNr. *A–D*, Mean profiles of $[5\text{-HT}]_o$ versus time evoked by 20 pulses (p) at 100 Hz (solid bar) expressed as a percentage of mean peak control either in control or the SERT inhibitor citalopram (*A*; 75 nM), the DAT inhibitor GBR 12909 (*B*; 1 μM), the Na_V^+ channel inhibitor TTX (*C*; 1 μM), or Ca^{2+}-free aCSF (*D*). *A*, Citalopram enhanced the extracellular lifetime of 5-HT and significantly enhanced mean peak $[5\text{-HT}]_o$ to 290 ± 18% of control (M-WU; $^{***}p < 0.001$; $n = 28$). *B*, GBR 12909 did not modify lifetime or mean peak $[5\text{-HT}]_o$ (M-WU; $p > 0.05$; $n = 14$). *C*, TTX abolished evoked 5-HT release (M-WU; $^{***}p < 0.001$; $n = 18$). *D*, 5-HT release was reversibly abolished in Ca^{2+}-free aCSF (M-WU; $^{***}p < 0.001$; $n = 12$). *E*, Mean peak $[5\text{-HT}]_o$ varied significantly with frequency (20 pulses; one-way ANOVA, $p < 0.001$) in a biphasic manner (Dunnett's *t* tests; asterisks denote *p* values vs 10 Hz: $^{*}p < 0.05$, $^{**}p < 0.01$, $^{***}p < 0.001$). *F*, Mean peak $[5\text{-HT}]_o$ varied significantly with pulse number (100 Hz; one-way ANOVA, $p < 0.001$) in a linear manner for pulse numbers <30 (linear regression with *y*-intercept = 0, dotted line; $R^2 = 0.97$).

(M-WU; $p < 0.001$; $n = 18–22$) and reversibly abolished with application of Ca^{2+}-free–EGTA-containing aCSF (Fig. 3*D*) (M-WU; $p < 0.001$; $n = 12$). Mean peak-evoked $[5\text{-HT}]_o$ varied significantly with frequency across the range of 10 to 200 Hz (20 pulses; one-way ANOVA; $p < 0.001$) in a biphasic manner that indicated frequency dependence at <100 Hz but a diminished ability to follow frequencies greater than this (Fig. 3*E*) (*post hoc* Dunnett's *t* tests vs 10 Hz: 20–100 Hz, $p < 0.001–0.05$; 200 Hz, $p > 0.05$). Mean peak-evoked $[5\text{-HT}]_o$ varied significantly with the number of pulses in a train (100 Hz; one-way ANOVA; $p < 0.001$) as observed previously (Iravani and Kruk, 1997; Bunin et al., 1998), showing a linear dependence at pulse numbers <30 (Fig. 3*F*) (linear regression over 0–30 pulses; *y*-intercept = 0; $R^2 = 0.97$). Trains of 20 pulses at 100 Hz were selected for all subsequent pharmacological investigations.

H_3R effects on 5-HT release in the SNr

Mean peak evoked $[5\text{-HT}]_o$ (20 pulses at 100 Hz) was significantly attenuated by bath application of selective H_3R agonists (*R*)-(-)-α-methylhistamine (R-mHA) or immepip (Fig. 4*A*,*B*) (Kruskal-Wallis, $p < 0.001$; $n = 14–15$). Each drug demonstrated a concentration-dependent inhibition of 5-HT release of up to 49 ± 5% of control by R-mHA (1 μM; $n = 14$) and to 39 ± 3% by immepip (5 μM; $n = 15$) with IC_{50} values of 23 nM (R-mHA; 95% confidence interval range, 13–43 nM; Hill slope, −1.1) and 43 nM, respectively (immepip; 95% confidence interval range, 20–95 nM; Hill slope, −0.73, not significantly different from 1.0). These IC_{50} values were not significantly different from one another ($p > 0.05$).

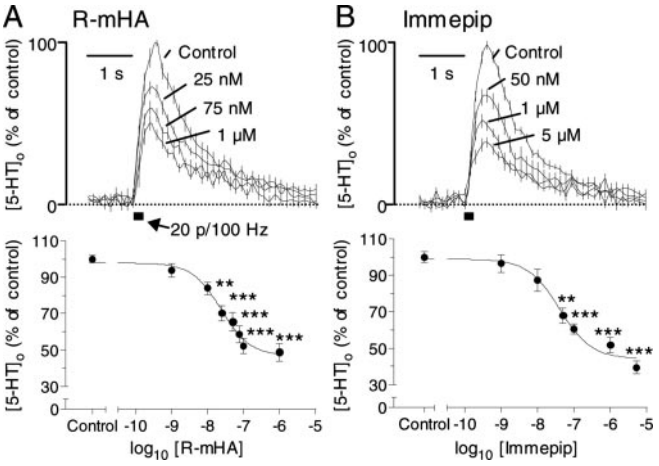

Figure 4. Dose-dependent inhibition of 5-HT release in SNr by H_3R agonists R-mHA and immepip. *A*, *B*, Top, Mean profiles of $[5\text{-HT}]_o$ versus time evoked by 20 pulses at 100 Hz (solid bar) expressed as a percentage of mean peak control. Bottom, Dose–response curves for mean peak $[5\text{-HT}]_o$ expressed as a percentage of mean peak control for R-mHA (*A*) or immepip (*B*). *A*, R-mHA dose dependently inhibited $[5\text{-HT}]_o$ ($n = 14–15$, Kruskal-Wallis; Dunn's *t* test vs control, $^{**}p < 0.01$, $^{***}p < 0.001$) with an IC_{50} value of 23 nM (95% confidence interval range, 13–43 nM; $R^2 = 0.57$; Hill slope, −1.1). *B*, Immepip dose dependently inhibited $[5\text{-HT}]_o$ ($n = 14–19$, Kruskal-Wallis; Dunn's *t* test vs control, $^{**}p < 0.01$, $^{***}p < 0.001$) with an IC_{50} value of 43 nM (95% confidence interval range, 20–95 nM; $R^2 = 0.65$; Hill slope, −0.73; not significantly different from 1.0).

To confirm that the actions of these H_3R agonists were attributable to selective agonism at H_3Rs, their effects were assessed in the presence of a selective H_3R antagonist, thioperamide. Whereas R-mHA (100 nM) reduced mean peak $[5\text{-HT}]_o$ from 100 ± 2 to 52 ± 4% without thioperamide (Fig. 5*A*) (M-WU; $p < 0.001$), R-mHA did not modify mean peak $[5\text{-HT}]_o$ in the presence of thioperamide (Fig. 5*A*) (1 μM; 108 ± 13% in thioperamide only vs 94 ± 6% in thioperamide plus R-mHA; $n = 19–25$; M-WU; $p > 0.05$). Similarly, immepip (1 μM) reduced mean peak $[5\text{-HT}]_o$ from 100 ± 3 to 52 ± 4% without thioperamide (Fig. 5*B*) (M-WU; $p < 0.001$) but did not modify $[5\text{-HT}]_o$ in the presence of thioperamide (Fig. 5*B*) (10 μM; 108 ± 5% in thioperamide only vs 104 ± 6% in thioperamide plus immepip; $n = 16–22$; M-WU; $p > 0.05$). In contrast, the effect of R-mHA (1 μM) was not prevented by the presence of a 5-HT_{1B} receptor antagonist, isamoltane (Fig. 5*C*) (1 μM; 111 ± 11.0% in isamoltane only vs 54 ± 7% in isamoltane plus R-mHA; M-WU; $p < 0.001$; $n = 12–21$) at a concentration of isamoltane previously observed to block 5-HT_{1B} agonist effects (Davidson and Stamford, 1996).

Direct or indirect H_3R effects?

Studies were undertaken to explore whether H_3R-mediated inhibition of 5-HT release might be attributable to H_3Rs present on GABAergic or glutamatergic inputs to 5-HT terminals rather than on the 5-HT terminals themselves. The effects of the H_3R agonist R-mHA were investigated in the presence of mixtures of either GABA or glutamate receptor antagonists (ionotropic and metabotropic). Despite the application of the GABA receptor antagonists picrotoxin (PTX; $GABA_A$ receptor antagonist, 100 μM) and saclofen ($GABA_B$ receptor antagonist, 50 μM), R-mHA

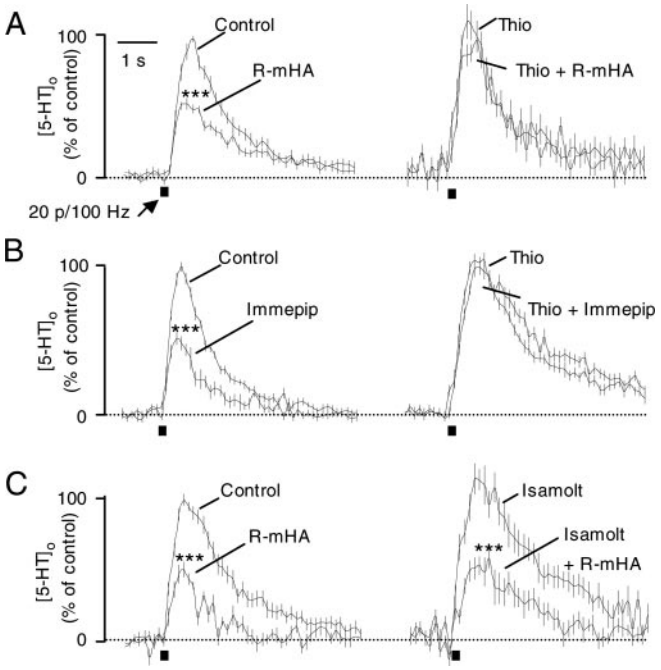

Figure 5. Inhibition of 5-HT release by H_3R agonists is caused by selective action at H_3Rs. *A–C*, Mean profiles of $[5\text{-HT}]_o$ versus time evoked by 20 pulses, 100 Hz (solid bar), expressed as a percentage of mean peak control in the absence (left) versus the presence (right) of the H_3R antagonist thioperamide (*A*, *B*) or the 5-HT_{1B} receptor antagonist isomoltane (*C*; 1 μM). In *A*, inhibition of peak $[5\text{-HT}]_o$ by R-mHA (100 nM, M-WU; $^{***}p < 0.001$; $n = 15$) was eliminated in the presence of thioperamide (1 μM; $n = 19–25$). *B*, Inhibition of peak $[5\text{-HT}]_o$ by immepip (1 μM, M-WU; $^{***}p < 0.001$; $n = 15$) was prevented when thioperamide was present (10 μM; $n = 16–22$). *C*, Inhibition of peak $[5\text{-HT}]_o$ by R-mHA (1 μM, M-WU; $^{***}p < 0.001$; $n = 12$) prevailed in the presence of 5-HT_{1B} antagonist isamoltane (1 μM, M-WU; $^{***}p < 0.001$; $n = 14–17$).

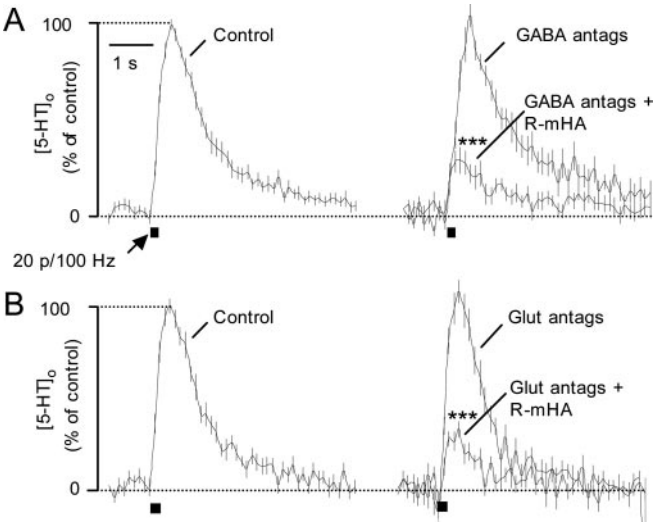

Figure 6. H_3R effects on 5-HT release occur during block of GABA or glutamate synapses. *A*, *B*, Mean profiles of $[5\text{-HT}]_o$ versus time evoked by 20 pulses, 100 Hz (solid bar), expressed as a percentage of mean peak control in the absence of drugs (left) or in the presence of antagonists (right) for GABA receptors (*A*) or glutamate receptors (*B*). *A*, Evoked $[5\text{-HT}]_o$ was not significantly modified by inclusion of GABA receptor antagonists (PTX, 100 μM; saclofen, 50 μM; $n = 12$). In the presence of GABA receptor block, R-mHA (1 μM) significantly diminished mean peak $[5\text{-HT}]_o$ (M-WU; $^{***}p < 0.001$; $n = 14$). *B*, Evoked $[5\text{-HT}]_o$ was not significantly modified by inclusion of glutamate receptor antagonists [(*S*)-MCPG, 200 μM; D-AP-5, 50 μM; GYKI 52466, 10 μM; $n = 12$]. In the presence of glutamate receptor block, R-mHA (1 μM) significantly diminished mean peak $[5\text{-HT}]_o$ (M-WU; $^{***}p < 0.001$; $n = 16$).

(1 μM) significantly inhibited mean peak $[5\text{-HT}]_o$ from 106 ± 6 to 27 ± 7% (Fig. 6*A*) (M-WU; $p < 0.001$; $n = 14–21$). Inhibition of 5-HT release via the H_3R also prevailed when R-mHA was applied in the presence of the glutamate receptor antagonists D-AP-5 (NMDA receptor antagonist, 50 μM), GYKI 52466 (noncompetitive AMPA/kainate receptor antagonist, 10 μM), and (*S*)-MCPG (Fig. 6*B*) (nonselective group I/II metabotropic glutamate receptor antagonist, 200 μM; 105 ± 6% in glutamate antagonists vs 30 ± 4% in glutamate antagonists plus R-mHA; M-WU; $p < 0.001$; $n = 16–26$). Statistical comparison of R-mHA effects in the absence versus the presence or either GABA or glutamate receptor antagonists (using recording sites matched for concentration of 5-HT released in drug-free controls) does not reveal a significant effect of synaptic block on R-mHA effects (M-WU; $n = 14–16$).

Discussion

5-HT detection in SNr

The evoked neurotransmitter release detected in the SNr in this study was Na_V^+ and Ca^{2+} dependent and sensitive to depolarization frequency and pulse number, as previously reported for 5-HT exocytosis in the SNr (O'Connor and Kruk, 1991; Iravani and Kruk, 1997; Bunin et al., 1998). It is well established that 5-HT is the predominant monoamine detected by FCV at CFMs in the rat SNr (Cragg et al., 1997b; Iravani and Kruk, 1997; Bunin et al., 1998); this differs from the guinea pig SNr in which 5-HT is detected far less frequently and DA predominates (Cragg et al., 1997b). Several lines of evidence indicate that the signal monitored in this study was indeed caused by the release of 5-HT. First, immunocytochemistry showed that serotonergic processes are abundant throughout the SNr. Second, the voltammograms resulting from the evoked release indicated that the released substance was identical in its electrochemical profile to the indoleamine 5-HT and not to the catecholamine DA. Third, inhibition of the SERT but not the DAT prolonged the extracellular lifetime and enhanced the peak amplitude of the 5-HT-like signal. These observations indicate that the electrochemical signal was attributable to 5-HT, with negligible contribution from DA, and confirm that the SERT participates in $[5\text{-HT}]_o$ regulation in the SNr as reported previously (Iravani and Kruk, 1997; Bunin et al., 1998).

H_3R control of 5-HT release in the SNr

In the present study, the evoked release of 5-HT in SNr was potently inhibited by the H_3R agonists R-mHA or immepip to levels that were <50% of those seen in controls. This attenuation of 5-HT release was dose dependent, with IC_{50} values for R-mHA and immepip that were consistent with previously reported values for H_3R efficacy in guinea pig ileum (Hew et al., 1990) and inhibition of striatal glutamate release (Molina-Hernandez et al., 2001), respectively. The inhibition of 5-HT release in SNr by activation of H_3Rs was confirmed further by experiments with the selective H_3R antagonist thioperamide. Previous application of thioperamide prevented the inhibition of 5-HT release by R-mHA or immepip. In contrast, the action of these H_3R agonists was not modified by antagonism of 5-HT_{1B} receptors, a 5-HT receptor type that has been shown to participate in presynaptic autoreceptor control of 5-HT release elsewhere in the brain (Barnes and Sharp, 1999). This observation indicates that the actions of the H_3 agonists were not attributable to effects on 5-HT autoreceptors.

The potent inhibition of 5-HT signaling by H_3Rs identifies a powerful role for these abundant receptors in the SNr (Pillot et al., 2002). Although H_3R-dependent regulation of 5-HT signal-

ing has been identified previously in rat cortex (Schlicker et al., 1988; Fink et al., 1990), the current data are the first to identify a comparable mechanism within the basal ganglia.

H_3R on GABA and glutamate synapses

To date, there is no anatomical information available regarding the specific identity of the neurons that express H_3Rs in the SNr and the ultrastructural location of these receptors. Thus, the synaptic circuitry by which H_3Rs detected in the SNr by radioligand binding (Pillot et al., 2002) can regulate 5-HT release is unidentified. Because *in situ* hybridization for mRNA for H_3Rs reveals only low expression within the SN (Pillot et al., 2002), the abundant H_3Rs in SN are unlikely to be expressed or localized on DA neurons in the SNc or on local or projection neurons within the SNr. However, moderate H_3R transcript expression has been identified in the raphe nuclei (Pillot et al., 2002); therefore, it is plausible that the H_3Rs are synthesized by 5-HT neurons and located on 5-HT terminals.

Because a similar level of H_3R mRNA expression has also been identified in the dorsal striatum, subthalamic nucleus, and pedunculopontine nucleus (Pillot et al., 2002), regions that send major non-5-HT projections (e.g., GABAergic or glutamatergic) to the SNr, we evaluated whether such inputs to the SNr might be involved in H_3R-mediated inhibition of 5-HT release. Previous evidence has indicated that H_3Rs in the SNr inhibit GABA release (Garcia et al., 1997; Garcia-Ramirez et al., 2004). The possibility that H_3Rs present on GABAergic or glutamatergic terminals in the SNr contribute to H_3R-mediated regulation of 5-HT release was investigated using receptor antagonists for GABA or glutamate. H_3R-mediated inhibition of 5-HT release was preserved in the presence of GABA–glutamate synaptic block; thus, a role for H_3Rs on GABA or glutamate terminals in this context seems unlikely. Furthermore, because in the absence of H_3R agonists neither GABA nor glutamate antagonists significantly modified $[5\text{-HT}]_o$, the control of 5-HT release in this paradigm does not appear to be under direct control by glutamate or GABA synapses. Whether the inhibitory action of H_3R agonists on GABA release in the SNr (Garcia et al., 1997; Garcia-Ramirez et al., 2004) is mediated via effects on 5-HT release remains to be tested.

The present results raise the possibility that the H_3R-mediated inhibition of 5-HT release is attributable to a direct action on 5-HT terminals via H_3Rs. This regulation of 5-HT release is noteworthy in light of reports indicating little, if any, regulation of 5-HT release in the SNr by 5-HT_{1B} autoreceptors (Nissbrandt et al., 1992; Iravani and Kruk, 1997). Despite a high density of 5-HT_{1B} receptors in the SNr, they are observed predominantly on striatonigral GABAergic terminals from the striatum rather than on serotonergic terminals (Boschert et al., 1994; Sari et al., 1999). It appears that 5-HT release in the SNr is not regulated by 5-HT receptors; this is not the case in the raphe nuclei where a plurality of 5-HT receptors perform autoreceptor-like functions (Stamford et al., 2000; Hopwood and Stamford, 2001). H_3R-mediated control of 5-HT release in SNr may provide a substitute mechanism for presynaptic inhibition of 5-HT release.

Conclusions

The present findings indicate a similar distribution of histaminergic and serotonergic processes in the SNr. Double-label immunohistochemical studies at the electronmicroscopic level will be required to establish whether there are histaminergic synapses on serotonergic terminals at this site. The results of the FCV studies are certainly consistent with an interaction between histaminergic and serotonergic systems. Thus, the data indicate that H_3Rs mediate presynaptic regulation of 5-HT release in the SNr. The location of the H_3Rs in question does not appear to involve either GABA or glutamate synapses; nevertheless, their possible presence on the terminals of other (e.g., cholinergic) projections to the SN cannot be discounted. The notion that the H_3Rs mediating inhibition of 5-HT release are located directly on 5-HT axons is consistent with the expression of the mRNA for H_3R in the raphe nuclei (Pillot et al., 2002) and the similar anatomical distribution of HA-immunoreactive and 5-HT-immunoreactive varicosities in the SNr. Given the apparent lack of autoreceptor control of 5-HT release at this site (Nissbrandt et al., 1992; Iravani and Kruk, 1997), H_3R activation may be a key mechanism for 5-HT regulation.

The significance of H_3R-mediated control of 5-HT release depends on the function(s) of 5-HT in the SNr. Serotonergic inputs to the SNr (Corvaja et al., 1993; Moukhles et al., 1997) have the potential to modify motor output signals (Jacobs and Fornal, 1993; Rick et al., 1995). Moreover, 5-HT is a target for therapeutic intervention regarding unwanted side effects associated with long-term DA replacement in PD, such as the wearing-off phenomenon and L-3,4-dihydroxyphenylalanine (L-DOPA)-induced dyskinesia (Nicholson and Brotchie, 2002). 5-HT_{2C} receptors on SNr projection neurons are excitatory (Rick et al., 1995); their binding is increased in the SNr of PD patients with L-DOPA-induced dyskinesia, suggesting a possible compensatory upregulation of receptors in response to decreased endogenous ligand (Fox and Brotchie, 2000). In this context, it should be noted that the selective serotonin reuptake inhibitor, fluoxetine, reduces dyskinesias in PD patients (Durif et al., 1995).

The capacity of HA to regulate 5-HT transmission in the SNr via H_3Rs may provide an attractive nondopaminergic target for improving therapies for PD. Identifying novel approaches to manipulate 5-HT neurotransmission may help to enhance the efficacy of current treatments not only for PD but also for mood disorders such as depression and anxiety, in which serotonergic manipulation is pivotal.

References

Adams JC (1992) Biotin amplification of biotin and horseradish peroxidase signals in histochemical stains. J Histochem Cytochem 40:1457–1463.

Alexander GE, Crutcher MD (1990) Functional architecture of basal ganglia circuits: neural substrates of parallel processing. Trends Neurosci 13:266–271.

Anichtchik OV, Rinne JO, Kalimo H, Panula P (2000a) An altered histaminergic innervation of the substantia nigra in Parkinson's disease. Exp Neurol 163:20–30.

Anichtchik OV, Huotari M, Peitsaro N, Haycock JW, Mannisto PT, Panula P (2000b) Modulation of histamine H3 receptors in the brain of 6-hydroxydopamine-lesioned rats. Eur J Neurosci 12:3823–3832.

Anichtchik OV, Peitsaro N, Rinne JO, Kalimo H, Panula P (2001) Distribution and modulation of histamine H(3) receptors in basal ganglia and frontal cortex of healthy controls and patients with Parkinson's disease. Neurobiol Dis 8:707–716.

Arias-Montano JA, Floran B, Garcia M, Aceves J, Young JM (2001) Histamine H(3) receptor-mediated inhibition of depolarization-induced, dopamine D(1) receptor-dependent release of [(3)H]-gamma-aminobutryic acid from rat striatal slices. Br J Pharmacol 133:165–171.

Arrang JM, Garbarg M, Schwartz JC (1983) Auto-inhibition of brain histamine release mediated by a novel class (H3) of histamine receptor. Nature 302:832–837.

Arrang JM, Drutel G, Schwartz JC (1995) Characterization of histamine H3 receptors regulating acetylcholine release in rat entorhinal cortex. Br J Pharmacol 114:1518–1522.

Barnes NM, Sharp T (1999) A review of central 5-HT receptors and their function. Neuropharmacology 38:1083–1152.

Boschert U, Amara DA, Segu L, Hen R (1994) The mouse 5-hydroxytryptamine1B receptor is localized predominantly on axon terminals. Neuroscience 58:167–182.

Brown RE, Haas HL (1999) On the mechanism of histaminergic inhibition of glutamate release in the rat dentate gyrus. J Physiol (Lond) 515:777–786.

Brown RE, Reymann KG (1996) Histamine H3 receptor-mediated depression of synaptic transmission in the dentate gyrus of the rat *in vitro*. J Physiol (Lond) 496:175–184.

Bunin MA, Prioleau C, Mailman RB, Wightman RM (1998) Release and uptake rates of 5-hydroxytryptamine in the dorsal raphe and substantia nigra reticulata of the rat brain. J Neurochem 70:1077–1087.

Corvaja N, Doucet G, Bolam JP (1993) Ultrastructure and synaptic targets of the raphe-nigral projection in the rat. Neuroscience 55:417–427.

Cragg S, Rice ME, Greenfield SA (1997a) Heterogeneity of electrically evoked dopamine release and reuptake in substantia nigra, ventral tegmental area, and striatum. J Neurophysiol 77:863–873.

Cragg SJ, Hawkey CR, Greenfield SA (1997b) Comparison of serotonin and dopamine release in substantia nigra and ventral tegmental area: region and species differences. J Neurochem 69:2378–2386.

Cragg SJ, Hille CJ, Greenfield SA (2002) Functional domains in dorsal striatum of the nonhuman primate are defined by the dynamic behavior of dopamine. J Neurosci 22:5705–5712.

Davidson C, Stamford JA (1996) Serotonin efflux in the rat ventral lateral geniculate nucleus assessed by fast cyclic voltammetry is modulated by 5-HT1B and 5-HT1D autoreceptors. Neuropharmacology 35:1627–1634.

Durif F, Vidailhet M, Bonnet AM, Blin J, Agid Y (1995) Levodopa-induced dyskinesias are improved by fluoxetine. Neurology 45:1855–1858.

Fink K, Schlicker E, Neise A, Gothert M (1990) Involvement of presynaptic H3 receptors in the inhibitory effect of histamine on serotonin release in the rat brain cortex. Naunyn Schmiedebergs Arch Pharmacol 342:513–519.

Fox SH, Brotchie JM (2000) 5-HT2C receptor binding is increased in the substantia nigra pars reticulata in Parkinson's disease. Mov Disord 15:1064–1069.

Garcia M, Floran B, Arias-Montano JA, Young JM, Aceves J (1997) Histamine H3 receptor activation selectively inhibits dopamine D1 receptor-dependent [3H]GABA release from depolarization-stimulated slices of rat substantia nigra pars reticulata. Neuroscience 80:241–249.

Garcia-Ramirez M, Aceves J, Arias-Montano J-A (2004) Intranigral injection of the H3 agonist immepip and systemic apomorphine elicit ipsilateral turning behaviour in naive rats, but reduce contralateral turning in hemiparkinsonian rats. Behav Brain Res 154:409–415.

Giorgetti M, Bacciottini L, Bianchi L, Giovannini MG, Cecchi M, Blandina P (1997) GABAergic mechanism in histamine H3 receptor inhibition of K(+)-evoked release of acetylcholine from rat cortex *in vivo*. Inflamm Res 46 [Suppl 1]:S33–S34.

Hew RW, Hodgkinson CR, Hill SJ (1990) Characterization of histamine H3-receptors in guinea-pig ileum with H3-selective ligands. Br J Pharmacol 101:621–624.

Hopwood SE, Stamford JA (2001) Multiple 5-HT(1) autoreceptor subtypes govern serotonin release in dorsal and median raphe nuclei. Neuropharmacology 40:508–519.

Iravani MM, Kruk ZL (1997) Real-time measurement of stimulated 5-hydroxytryptamine release in rat substantia nigra pars reticulata brain slices. Synapse 25:93–102.

Jacobs BL, Fornal CA (1993) 5-HT and motor control: a hypothesis. Trends Neurosci 16:346–352.

Kalló I, Butler JA, Barkovics-Kallo M, Goubillon ML, Coen CW (2001) Oestrogen receptor beta-immunoreactivity in gonadotropin releasing hormone-expressing neurones: regulation by oestrogen. J Neuroendocrinol 13:741–748.

Liposits Z, Sherman D, Phelix C, Paull WK (1986) A combined light and electron microscopic immunocytochemical method for the simultaneous localization of multiple tissue antigens. Tyrosine hydroxylase immunoreactive innervation of corticotropin releasing factor synthesizing neurons in the paraventricular nucleus of the rat. Histochemistry 85:95–106.

Molina-Hernandez A, Nunez A, Sierra JJ, Arias-Montano JA (2001) Histamine H3 receptor activation inhibits glutamate release from rat striatal synaptosomes. Neuropharmacology 41:928–934.

Moukhles H, Bosler O, Bolam JP, Vallee A, Umbriaco D, Geffard M, Doucet G (1997) Quantitative and morphometric data indicate precise cellular interactions between serotonin terminals and postsynaptic targets in rat substantia nigra. Neuroscience 76:1159–1171.

Nicholson SL, Brotchie JM (2002) 5-hydroxytryptamine (5-HT, serotonin) and Parkinson's disease–opportunities for novel therapeutics to reduce the problems of levodopa therapy. Eur J Neurol 9 [Suppl 3]:1–6.

Nissbrandt H, Waters N, Hjorth S (1992) The influence of serotoninergic drugs on dopaminergic neurotransmission in rat substantia nigra, striatum and limbic forebrain *in vivo*. Naunyn Schmiedebergs Arch Pharmacol 346:12–19.

O'Connor JJ, Kruk ZL (1991) Frequency dependence of 5-HT autoreceptor function in rat dorsal raphe and suprachiasmatic nuclei studied using fast cyclic voltammetry. Brain Res 568:123–130.

Panula P, Yang HY, Costa E (1984) Histamine-containing neurons in the rat hypothalamus. Proc Natl Acad Sci USA 81:2572–2576.

Panula P, Pirvola U, Auvinen S, Airaksinen MS (1989) Histamine-immunoreactive nerve fibers in the rat brain. Neuroscience 28:585–610.

Paxinos G, Watson C (1982) The rat brain in stereotaxic coordinates. Sydney: Academic.

Pillot C, Heron A, Cochois V, Tardivel-Lacombe J, Ligneau X, Schwartz JC, Arrang JM (2002) A detailed mapping of the histamine H(3) receptor and its gene transcripts in rat brain. Neuroscience 114:173–193.

Prast H, Tran MH, Fischer H, Kraus M, Lamberti C, Grass K, Philippu A (1999) Histaminergic neurons modulate acetylcholine release in the ventral striatum: role of H3 histamine receptors. Naunyn Schmiedebergs Arch Pharmacol 360:558–564.

Prell GD, Hough LB, Khandelwal J, Green JP (1996) Lack of a precursor-product relationship between histamine and its metabolites in brain after histidine loading. J Neurochem 67:1938–1944.

Rice ME, Nicholson C (1989) Measurement of nanomolar dopamine diffusion using low-noise perfluorinated ionomer coated carbon fiber microelectrodes and high-speed cyclic voltammetry. Anal Chem 77:1805–1810.

Rick CE, Stanford IM, Lacey MG (1995) Excitation of rat substantia nigra pars reticulata neurons by 5-hydroxytryptamine *in vitro*: evidence for a direct action mediated by 5-hydroxytryptamine2C receptors. Neuroscience 69:903–913.

Ryu JH, Yanai K, Watanabe T (1994) Marked increase in histamine H3 receptors in the striatum and substantia nigra after 6-hydroxydopamine-induced denervation of dopaminergic neurons: an autoradiographic study. Neurosci Lett 178:19–22.

Sari Y, Miquel MC, Brisorgueil MJ, Ruiz G, Doucet E, Hamon M, Verge D (1999) Cellular and subcellular localization of 5-hydroxytryptamine1B receptors in the rat central nervous system: immunocytochemical, autoradiographic and lesion studies. Neuroscience 88:899–915.

Schlicker E, Betz R, Gothert M (1988) Histamine H3 receptor-mediated inhibition of serotonin release in the rat brain cortex. Naunyn Schmiedebergs Arch Pharmacol 337:588–590.

Schlicker E, Fink K, Hinterthaner M, Gothert M (1989) Inhibition of noradrenaline release in the rat brain cortex via presynaptic H3 receptors. Naunyn Schmiedebergs Arch Pharmacol 340:633–638.

Schlicker E, Behling A, Lummen G, Gothert M (1992) Histamine H3A receptor-mediated inhibition of noradrenaline release in the mouse brain cortex. Naunyn Schmiedebergs Arch Pharmacol 345:489–493.

Schlicker E, Fink K, Detzner M, Gothert M (1993) Histamine inhibits dopamine release in the mouse striatum via presynaptic H3 receptors. J Neural Transm Gen Sect 93:1–10.

Schlicker E, Werthwein S, Zentner J (1999) Histamine H3 receptor-mediated inhibition of noradrenaline release in the human brain. Fundam Clin Pharmacol 13:120–122.

Schwartz JC, Lampart C, Rose C (1972) Histamine formation in rat brain *in vivo*: effects of histidine loads. J Neurochem 19:801–810.

Stamford JA, Davidson C, McLaughlin DP, Hopwood SE (2000) Control of dorsal raphe 5-HT function by multiple 5-HT(1) autoreceptors: parallel purposes or pointless plurality? Trends Neurosci 23:459–465.

Venton BJ, Michael DJ, Wightman RM (2003) Correlation of local changes in extracellular oxygen and pH that accompany dopaminergic terminal activity in the rat caudate-putamen. J Neurochem 84:373–381.

Vizuete ML, Traiffort E, Bouthenet ML, Ruat M, Souil E, Tardivel-Lacombe J, Schwartz JC (1997) Detailed mapping of the histamine H2 receptor and its gene transcripts in guinea-pig brain. Neuroscience 80:321–343.

Yamamoto Y, Mochizuki T, Okakura-Mochizuki K, Uno A, Yamatodani A (1997) Thioperamide, a histamine H3 receptor antagonist, increases GABA release from the rat hypothalamus. Methods Find Exp Clin Pharmacol 19:289–298.